MARR-HILDRETH ENHANCEMENT OF NDE IMAGES

B.G. Frock†

University of Dayton
Research Institute
Dayton, Ohio 45469

P. Karpur ‡

Systran Corporation
4126 Linden Avenue
Dayton, Ohio 45432

INTRODUCTION

Previous publications [1-5] have demonstrated the usefulness of digital image enhancement techniques for improving visual detection and resolution of features in NDE images. Many of the techniques are high-pass spatial domain convolution filters [6] which are used to enhance the appearance of edges by removing blur. Two of the major advantages of the more popular edge enhancement operators are their ease of implementation and their rapidity of execution [7]. This makes them very useful for rapid "screening" of images. Their major disadvantages are that they emphasize "noise" as well as edges, and some are directionally dependent operators which tend to suppress features that are not aligned in the "preferred" direction.

The problems of preferred orientation and noise enhancement can be minimized if "restoration" techniques such as Wiener deconvolutions [8] are applied. Unfortunately, these techniques are usually computationally intensive and, when applied in the two-dimensional Fourier domain, require highly specialized software that may be expensive or difficult to implement. Implementation of the two-dimensional Wiener deconvolution technique in small computers often requires that the size of the image be severely restricted.

The Marr-Hildreth operator was developed for detection of the intensity changes [9] in images. As Marr and Hildreth demonstrated, this bandpass operator is an optimal tradeoff between the high spatial frequency emphasis necessary for edge enhancement and the high spatial frequency attenuation necessary for noise suppression. Since it can be implemented as a convolution operator in the spatial domain, it can be applied without highly specialized software. The convolution should execute rapidly so long as the "size" of the Marr-Hildreth operator is small. The ease of implementation, rapidity of execution, lack of "preferred" orientation and ability to enhance edges in the presence of noise should make it useful for rapid enhancement of images prior to attempting more difficult and time-consuming techniques.

MARR-HILDRETH OPERATOR

This operator is the two-dimensional second derivative (Laplacian) of a two-dimensional Gaussian. The equation in rectangular coordinates is:

$$MH = A^{*}\left\{\left(\frac{X-\mu_x}{\sigma_x^2}\right)^2+\left(\frac{Y-\mu_y}{\sigma_y^2}\right)^2-\frac{1}{\sigma_x^2}-\frac{1}{\sigma_y^2}\right\}e^{-\frac{1}{2}\left[\left(\frac{X-\mu_x}{\sigma_x}\right)^2+\left(\frac{Y-\mu_y}{\sigma_y}\right)^2\right]} \quad (1)$$

where μ_x and μ_y are the mean values in the X-direction and the Y-direction, σ_x and σ_y are the standard deviations in the X-direction and the Y-direction, and "A" is a multiplicative constant. The shapes and bandwidths of the filters in the frequency and spatial domains are controlled by the values of the standard deviations as is illustrated in Fig. 1. Small values for the standard deviations produce a narrow operator in the spatial domain and a broad operator in the frequency domain. This narrow spatial domain operator places more emphasis on the higher frequencies. A narrow spatial domain operator will be very effective for removing blur from an image, but may amplify high spatial frequency noise. Large values for the standard deviations result in a broad operator in the spatial domain and a narrow operator in the frequency domain. The broad spatial domain operator places more emphasis on the lower freqeuncies. Such an operator will remove less blur from an image, but will also not amplify high frequency noise.

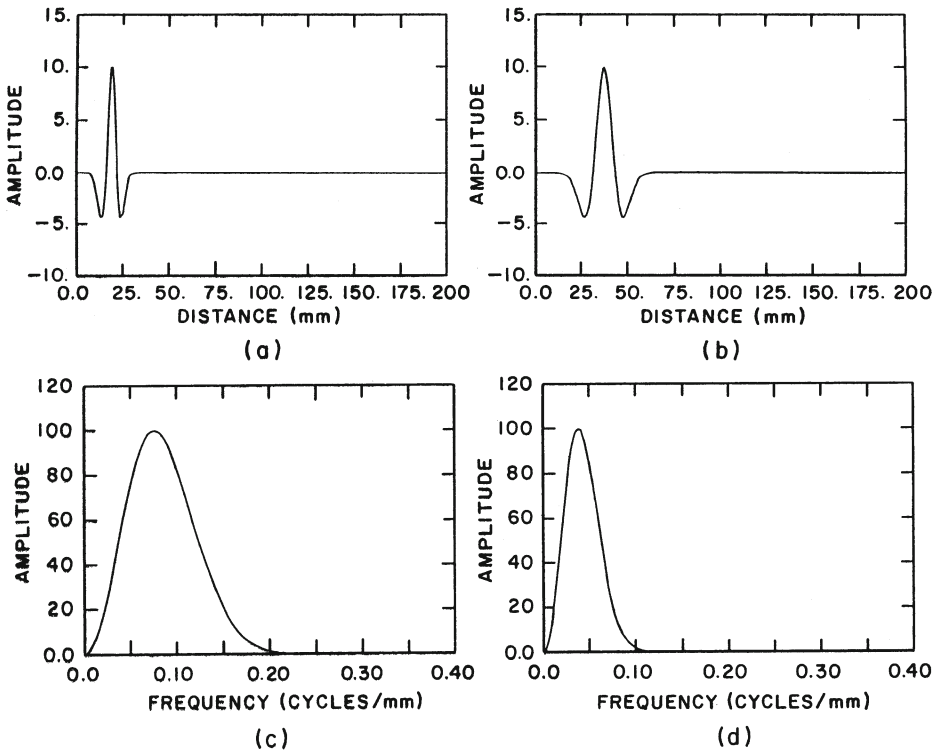

Fig. 1. Marr-Hildreth convolution operators: (a) Spatial Domain, $\sigma = 3$; (b) Spatial Domain, $\sigma = 6$; (c) Fourier amplitude spectra of "a"; (d) Fourier amplitude spectra of "b".

DATA ACQUISITION

Experimental Data

Ultrasonic C-scan data were acquired from a 32-ply thick graphite epoxy composite panel. A computer controlled, immersion C-scanning technique was used to acquire, digitize and store ultrasonic data from 40,000 discrete points on the sample. These discrete points were separated by 0.025mm in the two orthogonal directions. The sample was insonified with a Precision Acoustic Device low-frequency (3MHz) acoustic microscope transducer excited with a spike pulse and focused on the entry surface of the sample. Data were collected from a 120ns wide gate located over the first negative going cycle of the rf entry surface echo. The minimum value (sign included) in that gate was digitized and stored at each of the 40,000 discrete sampling points. The C-scan images generated from this data were essentially topographic maps of the sample's entry surface with depth variations encoded in the amplitude values at the discrete points. A magnified optical image of the sample's surface is shown in Fig. 2. The major surface topographic feature in the image is the weave pattern, i.e., the impression of the bleeder cloth used during fabrication.

Simulated Noise

Noisy data were generated by adding computer simulated noise to the nearly-noise-free experimental ultrasonic data. The amplitude of the noise was Gaussian distributed with the standard deviation set at 3.3% of the maximum amplitude value of the experimental data set.

One-Dimensional Simulated Data

Simulated studies of one-dimensional data were undertaken to help determine some of the capabilities and limitations of the Marr-Hildreth convolution operator. The studies consisted of simulating a sensor's point spread function with a one-dimensional Gaussian, and then convolving the point spread function with a one-dimensional "ideal" image feature to produce a simulated sensor-generated image. This simulated image was then convolved with Marr-Hildreth operators and the results were compared with results obtained by Wiener deconvolution of the Gaussian point spread function from the simulated sensor image.

RESULTS

Experimental Nearly-Noise-Free Data

Unenhanced ultrasonic data were used to generate the image in Fig. 3a. This image of the sample's entry surface is very blurred, and only portions of the weave pattern are visually resolvable. The results of applying

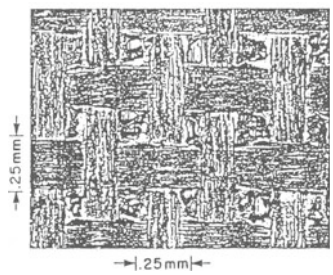

Fig. 2. Optical microscope image of graphite/epoxy sample's surface (Magnification = 50X).

Marr-Hildreth operators with different standard deviations (1.0 and 2.0 pixels) to the image data of Fig. 3a are shown in Figs. 3b and 3c. The weave pattern on the sample's surface is visually resolvable in both of these enhanced images. The effects of choosing different values for the standard deviations are also clearly evident in these images and in the pixel amplitude plots in Figs. 3e and 3f. The amplitude plots are from horizontal line 45 of each of the images in Figs. 3a, 3b and 3c. The Marr-Hildreth operator with the smaller standard deviation removes more blur, but also tends to emphasize more noise in the image. The use of a Marr-Hildreth operator with a larger standard deviation generates images with less noise, but less blur is removed form the images. The Marr-Hildreth convolutions were implemented as discrete 13 x 13 moving window operations. When performed on a MicroVax computer, the convolution operations on the 40,000 point images required about 200 seconds per image.

A two dimensional Fourier domain Wiener filter deconvolution [8] was applied to a portion of the ultrasonic data for comparative purposes. The point spread function of the transducer was generated from scans of a thin wire (0.076mm). The results of the Wiener deconvolution are displayed in Fig. 4a. This deconvolved image is visually similar to the images resulting form Marr-Hildreth convolutions (see Fig. 3). A plot of the pixel amplitudes from horizontal line 45 of the image in Fig. 4a is shown in Fig. 4b. This amplitude plot is also quite similar to that resulting from Marr-Hildreth convolutions (see Fig. 3).

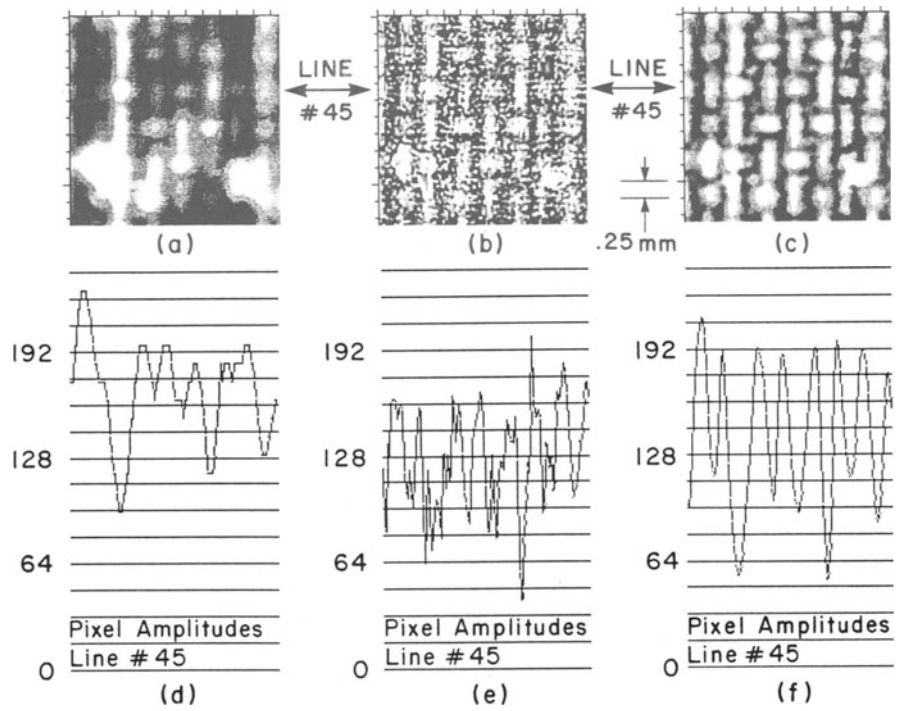

Fig. 3. Ultrasonic images of graphite/epoxy sample's surface: (a) Original data; (b) Marr-Hildreth operator (σ=1) convolved with "a"; (c) Marr-Hildreth operator (σ=2) convolved with "a"; (d) through (f) Pixel amplitudes along lines 45 of "a" through "c".

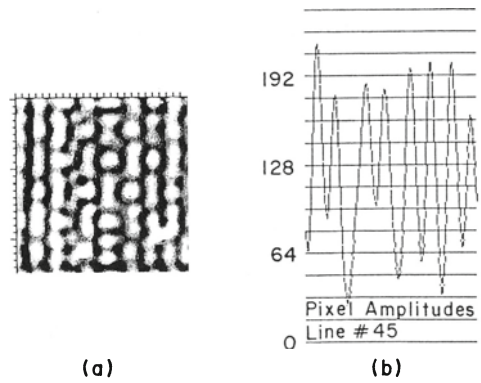

Fig. 4. Weiner deconvolution of data in Fig. 3a: (a) Deconvolved image; (b) Pixel amplitude plot from horizontal line 45 of "a".

Noisy Data

The results of adding Gaussian noise to the image in Fig. 3a are shown in Fig. 5a. The noise appears as isolated light and dark "speckles" in the image. Marr-Hildreth operators with different standard deviations (1 and 2 pixels) were convolved with the "noisy" data. The resulting images are presented in Figs. 5b and 5c. Amplitude plots from horizontal line number 45 for each of the images in Fig. 5 are also shown in Fig. 5. The narrower Marr-Hildreth operator (σ = 1) reduces the blur, but emphasizes the noise which is present in the data. The broader Marr-Hildreth operator (σ = 2) removes less blur, but also generates results with less noise. The amplitude plots in Figs. 5d, 5e, and 5f substantiate the visual interpretations of the images in Figs. 5a, 5b, and 5c.

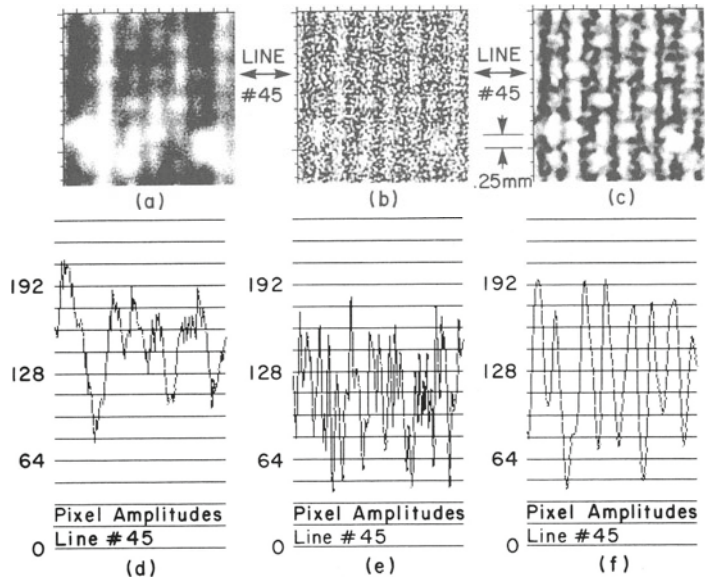

Fig. 5. "Noisy" image of graphite/epoxy sample's surface: (a) Unenhanced; (b) Marr-Hildreth operator (σ = 1) convolved with "a"; (c) Marr-Hildreth operator (σ = 2) convolved with "a"; (d) through (f) Pixel amplitudes along lines 45 of "a" through "c".

One-Dimensional Simulated Data

The Gaussian point spread function, an "ideal" image and the simulated sensor generated image are shown in Figs. 6a, 6b, and 6c respectively. The standard deviation of the point spread function was 5 mm and the "ideal" image consisted of 30 adjacent impulse spikes. Fig. 7a shows the results of convolving the Marr-Hildreth operator (σ = 3) with the simulated sensor generated image of Fig. 6c. The results of Wiener deconvolution of the point spread function (Fig. 6a) from the simulated sensor generated image of Fig. 6c are shown in Fig. 7b. The results of convolving the Marr-Hildreth operator with the simulated sensor generated image are illustrated in Fig. 7a. Some of the artifacts which might result from application of a Marr-Hildreth convolution operator are evident in Fig. 7a. There are deep negative troughs present on the outer edges of the feature, and there is a shallow trough in the center of the feature. The "deep" negative troughs on either side of the "feature" will appear in an image as dark colored bands at the boundaries of the "feature". This banding actually helps the visual/neural system detect [10] the "feature". The shallower trough which has been created in the center of the image "feature" might well result in the visual misinterpretation of the image "feature" as being two smaller features rather than the boundaries of a single larger feature.

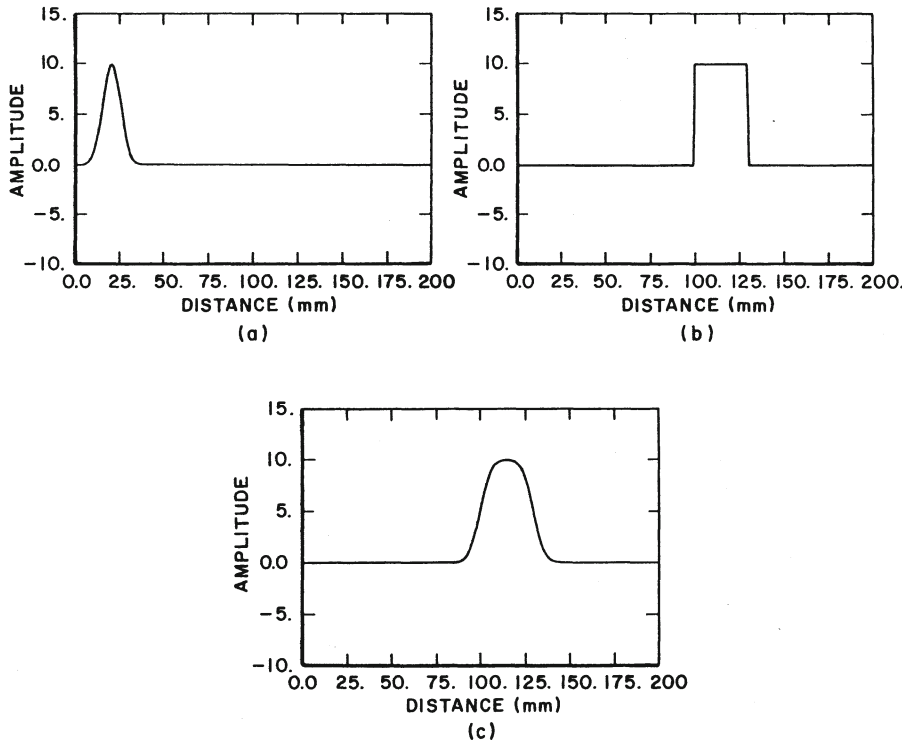

Fig. 6. Simulated feature: (a) Simulated point spread function of sensor; (b) Ideal feature; (c) Simulated sensor generated feature ("a" convolved with "b").

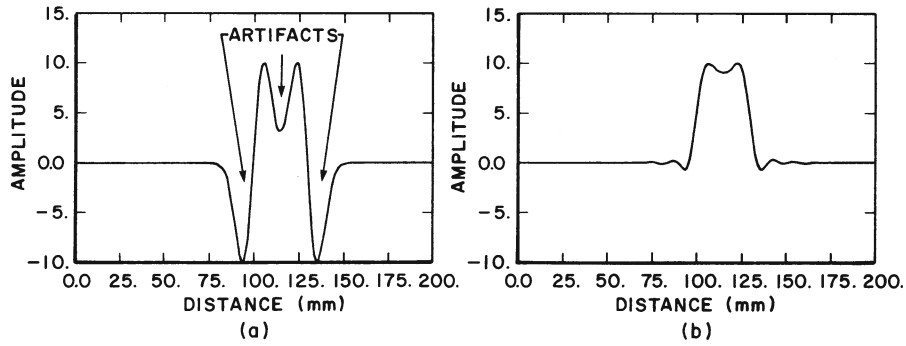

Fig. 7. Enhancement of a simulated sensor generated image: (a) Marr-Hildreth operator (σ=3) convolved with Fig. 6c; (b) Wiener deconvolution of Fig. 6c.

CONCLUSIONS

We have shown that the Marr-Hildreth operator can be used to remove blur in ultrasonic NDE images even in the presence of noise. It is easily implemented as a spatial domain convolution operator, and, as such does not require sophisticated or highly specialized software for its application. The spatial domain convolution executed rapidly, and in the case of the image data examined in this study, produced results similar to those achieved with a two-dimensional Fourier domain Wiener filter. We have also demonstrated that artifacting can occur with the application of the Marr-Hildreth operator and have attempted to explain how that artifacting might affect the visual interpretation of a Marr-Hildreth enhanced image. Despite this artifacting, the Marr-Hildreth operator can serve as a useful tool for the rapid enhancement of NDE images prior to the application of more sophisticated and time-consuming enhancement techniques.

ACKNOWLEDGEMENTS

† Research sponsored by the AFWAL/Materials Laboratory under Contract No. F33615-86-C-5016.

‡ Research sponsored by the AFWAL/Materials Laboratory under Contract No. F33615-88-C-5402.

The authors thank Mr. Richard Martin for implementation of the spatial domain Marr-Hildreth convolution operator.

REFERENCES

1. B. G. Frock and R. W. Martin, "Applications of Digital Image Enhancement Techniques for Improved Ultrasonic Imaging of Defects in Composite Materials," Review of Progress in Quantitative NDE, Vol. 6A, edited by D. O. Thompson and D. E. Chimenti, (Plenum Press, New York, New York, 1987), pp. 781-789.
2. M. J. Closier, "Automatic Product Analysis Using X-Rays," NDT International, 59-65 (1981).
3. M. H. Jacoby, R. S. Loe and P. A. Dondes, "Computer Evaluation of Real-Time X-Ray and Acoustic Images," SPIE, Applications of Digital Image Processing IV, Vol. 359, 273-277 (1982).

4. J. Boutin and C. Forget, "Powerful Image Analysis Techniques for Quantitative Measurements of Materials," Metal Progress, April 1988, pp. 24-55.
5. R. S. Gilmore, R. E. Joynson, C. R. Trzaskos and J. D. Young, "Accoustic Microscopy: Materials Art and Materials Science," Review of progress in Quantitative NDE, Vol. 6A, edited by D. O. Thompson and D. E. Chimenti, (Plenum Press, New York, New York, 1987), pp. 553-562.
6. L. S. Davis, "A Survey of Edge Detection Techniques," Computer Graphics and Image Processing, 4, 1975, pp. 248-270.
7. A. N. Venetsanopoulos and V. Cappellini, "Real-Time Image Processing," Multidimensional Systems, Techniques and Applications, edited by S. G. Tzafestas (Marcel Dekker, Inc., New York, New York, 1986), pp. 3345-399.
8. R. C. Gonzalez and P. Wintz, Digital Image Processing (Addison-Wesley Publishing Company, Reading, Massachusetts, 1977), pp. 210-211.
9. D. Marr and E. Hildreth, "Theory of Edge Detection," Proceedings of the Royal Society of London B, Vol. 207, 1980, pp. 187-217.
10. E. L. Hall, R. P. Kruger, S. J. Dwyer, D. L. Hall, R. W. McLaren and G. S. Lodwick, "A Survey of Preprocessing and Feature Extraction Techniques for Radiographic Images," IEEE Transactions on Computers, Vol. C-20, No. 9, September 1971, pp. 1032-1044.